



A new N₆ hexadentate ligand and a novel heptacoordinated N₆O-type Fe(III) compounds: Synthesis, characterization and structure of [Fe(dimpyen)(OH)](A)₂ (A = PF₆⁻ or ClO₄⁻)

Norma Ortega-Villar^a, Víctor M. Ugalde-Saldívar^a, Blas Flores-Pérez^a, Marcos Flores-Alamo^a, J.A. Real^b, Rafael Moreno-Esparza^{a,*}

^a Facultad de Química, Universidad Nacional Autónoma de México, México DF 04510, Mexico

^b Instituto de Ciencia Molecular (ICMol), Universidad de Valencia C/Catedrático José Beltrán Martínez, 2, Paterna, 46071 Valencia, Spain

ARTICLE INFO

Article history:

Received 21 December 2010
Received in revised form 29 April 2011
Accepted 6 May 2011
Available online 17 May 2011

Keywords:

Iron (III) complexes
Hexadentate ligand
Heptacoordination
Redox properties
Magnetic properties
Crystal structure

ABSTRACT

In this contribution, we report the syntheses of a novel N₆ donor set ligand, dimpyen = N1,N2-di[(1-methyl-1H-2-imidazolyl) methyl]-N1,N2-di(2-pyridylmethyl)-1,2-ethanediamine. This type of ligand was designed to modulate the properties of the metal ions bound to it. The reaction with Fe(II) gives off a new heptacoordinated iron(III) complex. We study the spectroscopic (UV–Vis), magnetic and electrochemical behavior and also made the structural determination with X-ray diffraction at 134 K and a heptacoordinated N₆O-type derivative of Fe(III) is reported as well. This complex crystallize as perchlorate or hexafluorophosphate and the formula of these derivatives are [Fe(dimpyen)(OH)](PF₆)₂ (**1**) and [Fe(dimpyen)(OH)](ClO₄)₂ (**2**) which both crystallize with an intermediate geometry, between pentagonal bipyramidal and monocapped octahedral. The UV–Vis spectra in CH₃CN solution show a shoulder at 306 nm assigned to one ligand–metal charge-transfer (LMCT) transition, in addition, a weaker and wide band assigned to the charge transfer HO–Fe transition (λ_{max} at 404 nm with an extinction coefficient of 818 cm⁻¹ M⁻¹) is also observed. The magnetic studies corroborate a high-spin iron (III) species in all the temperature range considered. Measurements of cyclic voltammetric confirm a reversible system Fe(III) species, with $E_{1/2} = -0.380$ V/Fc⁺–Fc, this low potential value explains the high stability of the Fe(III) and the easy oxidation of Fe(II) by atmospheric O₂(g) reaction.

© 2011 Elsevier B.V. All rights reserved.

1. Introduction

In recent years, considerable effort has been focused on the synthesis of molecular materials with Fe that exhibit physical properties that may be switched in a controlled manner, especially in the magnetochemical area, because they are potentially good candidates for signal generation and processing [1]. Such behavior is modulated with the type of ligand bound to either Fe(II) or Fe(III). Our group is involved with the design of new ligands to do this [2]. On the other hand, seven-coordination is not common in transition-metal chemistry: an estimate based on the number of transition-metal sigma-bonded complexes found in the Cambridge Structural Database reveals that heptacoordinate complexes represent only 1.8% of the total number of structures reported [3]. Being seven an odd coordination number, no regular polyhedron can describe the coordination sphere around the metal atom. The most common polyhedra have the pentagonal bipyramid or either the capped octahedron or the capped trigonal prism, types of vertices

in different proportions, which should allow for easy identification of the stereochemistry through NMR spectroscopy in solution or by infrared spectroscopy in the solid state [4]. However very often, it is possible to observe solution spectra consistent with seven equivalent ligands due to the existence of low energy barrier fluxional processes. These geometries are receiving more attention as they can be identified as intermediates in associated reactions of various six-coordinated complexes [5,6]. It is clear that single crystal X-ray crystallography should be better adapted to fully characterize the stereochemistry of a given heptacoordinate molecule.

Then heptacoordination is a well-known coordination mode, although examples with iron(II) or (III) are rather rare. Some are reported in compounds with iron(II), observed with pentadentate ligands maintaining five coordination sites in one plane and allowing two axial coordinations [7]. There are very few structural reports of an heptacoordinated Fe(III) [8].

Furthermore, the study of compounds with this geometry is also of interest from another point of view, since it has been found that Fe(III) PBP complexes with aza-ligands exhibit an excellent superoxide dismutase (SOD) activity and offer considerable promise as SOD catalysts for pharmaceutical applications. In these

* Corresponding author. Tel.: +52 (55) 56223793; fax: +52 (55) 56162019.

E-mail address: moresp@servidor.unam.mx (R. Moreno-Esparza).

systems, the $[\text{Fe}(\text{N}_5)(\text{H}_2\text{O})\text{OH}]$ form of the complex is responsible for the catalytic properties, and a condition for the high activity of the complexes is their existence in mostly this form under physiological pH conditions [9,10].

Although several reviews on this subject have been published lately, the ongoing study of these systems does not fail to provide novel and interesting information.

The analysis of such parameters as electrochemical behavior and UV–Vis spectroscopy should render more arguments to establish a relationship between the studied properties and the chemical behavior of these complexes [11].

In light of the aforementioned facts, we report the syntheses of a new N_6 donor set ligand dimpyen = N1,N2-di[(1-methyl-1H-2-imidazolyl)methyl]-N1,N2-di(2-pyridylmethyl)-1,2-ethanediamine, and the syntheses, spectroscopic (UV–Vis), magnetic and structural characterization of a novel heptacoordinated N_6O -type iron(III) complex with an intermediate geometry between pentagonal bipyramid and capped octahedron.

2. Materials and methods

2.1. Reagents and solvents

Starting reagents and solvents were purchased from commercial sources and used as received.

2.2. Physical measurements

Infrared spectra were recorded on a Perkin–Elmer/1600 FT IR spectrometer on KBr pellets in the 4000–450 cm^{-1} range. Elemental analyses were done on a Fisons elemental micro analyzer model EA 1108, CHNS-O. ^1H NMR spectroscopic measurements were done on Varian 300 NMR Unity-Inova spectrometer using TMS as internal standard. Mass spectroscopy (FAB+), was done in a JEOL JMS-SX spectrometer, 102 A. UV–visible spectra were recorded on a Diode array HP 8493A spectrophotometer at 293 K on 1.0 cm quartz cell.

2.2.1. Magnetic studies

The variable-temperature (1.8–300 K) magnetic susceptibility measurements for each Fe(III) derivative were recorded with a Quantum Design MPMS2SQUID susceptometer and calibrated with $(\text{NH}_4)_2\text{Mn}(\text{SO}_4)_2 \cdot 12\text{H}_2\text{O}$. In all cases the χ_M values have been corrected for diamagnetism.

2.2.2. Electrochemical measurements

All experiments were performed with an EG&G–PAR 263 A potentiostat-galvanostat in acetonitrile solution containing 0.1 M N-tetrabutylammonium hexafluorophosphate, $(\text{C}_4\text{H}_9)_4\text{NPF}_6$, as the supporting electrolyte. A typical three-electrode array was employed for all electrochemical measurements: glass carbon micro-disk (C, 7.1 mm^2) as working electrode, Pt wire as counter electrode, and a pseudoreference electrode of $\text{AgBr}(\text{s})-\text{Ag}(\text{wire})$ immersed in an acetonitrile 0.1 M $(\text{C}_4\text{H}_9)_4\text{NBr}$ solution. All solutions were deoxygenated with N_2 before each measurement. All voltammograms were started from the current null potential ($E_{i=0}$) of each solution and were scanned in both directions. In agreement with IUPAC convention [12], the voltammogram of the ferricinium/ferrocene (Fc^+/Fc) system, used as reference, was obtained to establish the values of half wave potentials ($E_{1/2}$) for each experiment from the expression $E_{1/2} = (E_{ap} + E_{cp})/2$.

2.2.3. Single crystal X-ray diffraction

X-ray data collection, structure solution and refinement were made from crystals of the complex suitable for diffraction obtained

from the reaction vessel. Diffraction experiments were performed on an Atlas (Gemini Mo) area detector diffractometer and analyzed using Mo $\text{K}\alpha$ X-ray radiation ($\lambda = 0.71073 \text{ \AA}$). The dimensions of the analyzed crystals were; $0.40 \times 0.37 \times 0.18 \text{ mm}$ for **1** and $0.45 \times 0.18 \times 0.06 \text{ mm}$ for **2**. Only random fluctuations of less than 2% in the intensities of three standard reflections were observed during the course of data collection. Neutral atom scattering factors and anomalous dispersion corrections were taken from International Tables for Crystallography [13]. The data were corrected for absorption effects using the analytical numeric absorption correction using a multifaceted crystal model based on expressions derived by Clark and Reid [14]. The structure was solved by direct methods using the program SIR-2004 [15] combined with Fourier difference syntheses and refined against F^2 , least-squares refinement based on F^2 was carried out by full-matrix method with SHELXL-97-2 [16]. All non-hydrogen atoms were refined anisotropically successfully, while hydrogen atoms were included at calculated positions by using the riding model. The crystal data for the analyzed compounds with other pertinent details for the structure determination are reported in Table 1 while the selected bond length and angles of the compound are presented in Table 2. Complete listings of bond lengths, bond angles, and anisotropic thermal parameters are supplied as supplementary material. The molecular structure drawings were generated using ORTEP for windows [17].

3. Experimental

3.1. Synthesis of the ligand dimpyen

The synthetic route of this new ligand is presented in the Scheme 1, and each stage of the procedure is presented below.

3.1.1. 1-Methyl-1H-imidazole-2-carbaldehyde (A)

1-Methyl-imidazole (3 mL, 0.038 mol) was dissolved in 25 mL of dry THF, under N_2 atmosphere, the system is cooled to -78°C and stirred for 10 min, to this is added slowly 6.6 mL of butyl-lithium (0.146 mol, 2.5 M in hexane) keeping the temperature below -73°C , after 5 min, 5.3 mL (0.076 mol) of dimethylformamide was added. This solution is stirred during 1 h at -73°C and then allowed to reach room temperature while stirring 40 min more. After this period, 189 mL HCl 2 N are added and stirred 1 h at room temperature. The mixture is then neutralized to pH 10 with 40% NaOH and then extracted with dichloromethane ($3 \times 60 \text{ mL}$). All organic extracts are collected and dried over Na_2SO_4 at reduced pressure. After distillation a colorless solid is obtained yielding 4.117 g (98.5%).

3.1.2. [(E)-[(1-Methyl-1H-imidazol-2-yl)methylidene]amino]ethylamine (B)

500 mg (4.54 mmol) of (A), 1.09 g (9.10 mmol) of MgSO_4 and 5 mL of dichloromethane were stirred under N_2 . To this mixture 0.151 mL (136.2 mg; 2.27 mmol) of ethylenediamine were dissolved in 1 mL of dichloromethane, and stirred overnight at room temperature. The mixture was filtered over cellulose and washed with dichloromethane ($3 \times 10 \text{ mL}$) and dried in vacuum, obtaining 400 mg (72.7%) of a colorless solid.

3.1.3. [(1-Methyl-4,5-dihydro-1H-imidazol-2-yl)methyl](2-[(1-methyl-4,5-dihydro-1H-imidazol-2-yl)methyl]amino)ethylamine (C)

200 mg (0.819 mmol) of (B) were dissolved in 15 mL of methanol, cooled in an ice bath and stirred. Then 0.062 mg (1.64 mmol) of sodium borohydride was added. After the solid dissolves the mixture is allowed to reach room temperature and stirred six more hours. After this period, NaCl saturated solution is added until precipitation and then extracted with chloroform ($4 \times 60 \text{ mL}$), the

Table 1
Crystal data and structure refinement for **1** and **2**.

Complex	1	2
Empirical formula	C ₂₄ H ₃₁ F ₁₂ Fe N ₈ O P ₂	C ₂₄ H ₃₁ Cl ₂ Fe N ₈ O ₉
Formula weight	793.36	702.32
Temperature (K)	134(2)	134(2)
Wavelength (Å)	0.71073	0.71073
Crystal system	triclinic	triclinic
Space group	P $\bar{1}$	P $\bar{1}$
Unit cell dimensions		
<i>a</i> (Å)	9.7670(10)	9.3300(10)
<i>b</i> (Å)	12.7260(10)	12.7310(10)
<i>c</i> (Å)	13.3260(10)	12.9760(10)
α (°)	76.354(4)	77.961(5)
β (°)	74.751(4)	72.203(6)
γ (°)	81.120(4)	81.945(6)
Volume (Å ³)	1545.4(2)	1430.4(2)
<i>Z</i>	2	2
<i>D</i> _{calc} (Mg/m ³)	1.705	1.631
Absorption coefficient (mm ⁻¹)	0.7	0.782
<i>F</i> (0 0 0)	806	726
Crystal size (mm ³)	0.40 × 0.37 × 0.18	0.45 × 0.18 × 0.06
θ Range for data collection (°)	3.2–27.08	3.19–27.11
Index ranges	–12 ≤ <i>h</i> ≤ 12, –13 ≤ <i>k</i> ≤ 16, –17 ≤ <i>l</i> ≤ 16	–11 ≤ <i>h</i> ≤ 10, –16 ≤ <i>k</i> ≤ 13, –16 ≤ <i>l</i> ≤ 16
Reflections collected	12396	12278
Independent reflections	6668 [<i>R</i> _(int) = 0.0192]	6141 [<i>R</i> _(int) = 0.0370]
Completeness to $\theta = 27.08^\circ$	98.1%	97.2%
Absorption correction	analytical	analytical
Maximum and minimum transmission	0.909 and 0.835	0.961 and 0.815
Refinement method	full-matrix least-squares on <i>F</i> ²	full-matrix least-squares on <i>F</i> ²
Data/restraints/parameters	6668/42/490	6141/2/400
Goodness-of-fit on <i>F</i> ²	1.098	1.085
Final <i>R</i> indices [<i>I</i> > 2 σ (<i>I</i>)]	<i>R</i> ₁ = 0.0389, <i>wR</i> ₂ = 0.1072	<i>R</i> ₁ = 0.0595, <i>wR</i> ₂ = 0.1742
<i>R</i> indices (all data)	<i>R</i> ₁ = 0.0498, <i>wR</i> ₂ = 0.1108	<i>R</i> ₁ = 0.0781, <i>wR</i> ₂ = 0.1864
Largest diff. peak and hole (e Å ⁻³)	0.641 and –0.663	0.770 and –1.273

resulting colorless solid is dried over Na₂SO₄ at reduced pressure with 67% yield (135 mg).

3.1.4. N1,N2-Di[(1-metil-1H-2-imidazolil)metil]-N1,N2-di(2-piridil-metil)-1,2-etanodiamina (dimpyen)

In a round bottom flask a mixture 100 mg (0.403 mmol) of (**C**), 132.2 mg (0.806 mmol) of picolyl chloride, 10 mL of toluene and 322 mg (8.05 mmol) of a NaOH in 5 mL water solution was refluxed 48 h. Then, the mixture was cooled in an ice bath were a slightly yellow precipitate was obtained. The precipitate was filtered and washed with water (3 × 10 mL) and methanol (3 × 10 mL) and dried at reduced pressure. The light yellow solid was separated by column chromatography (SiO₂/CHCl₃, CH₃OH, NH₄OH (60:6:0.6)) yielding 80% (141 mg).

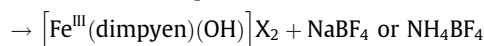
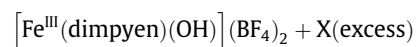
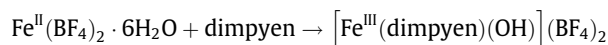
¹H NMR (300 MHz, CDCl₃) see Scheme 2: 8.51 (1H, d, *J*_{2–3} = 6 Hz, **H2**), 7.60 (1H, dd, *J*_{4–3} = 6 Hz, *J*_{4–5} = 6 Hz, **H4**), 7.29 (1H, d, *J*_{5–4} = 6 Hz, **H5**), 7.15 (1H, dd, *J*_{3–2} = 6 Hz, *J*_{3–4} = 6 Hz, **H3**), 6.88 (1H, s, **H12**), 6.77 (1H, s, **H11**), 3.69 (2H, s, **H9**), 3.67 (2H, s, **H7**), 3.51 (3H, s, **H13**), 2.65 (2H, s, **H8**).

3.2. Preparation of the coordination compounds

The synthesis of the reported complexes is achieved irrespective of either if Fe(II) or Fe(III) are used as starting material.

3.2.1. Synthesis with Fe(II) salt

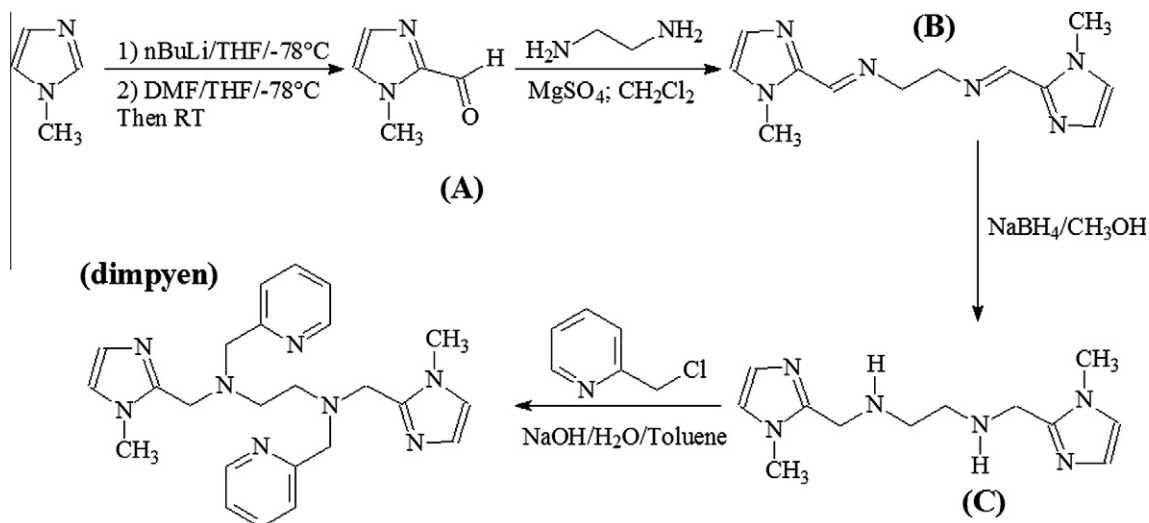
The synthetic procedure starting with Fe(II) is as follow:

**Table 2**
Selected bond lengths [Å] and angles [°] for **1** and **2**.

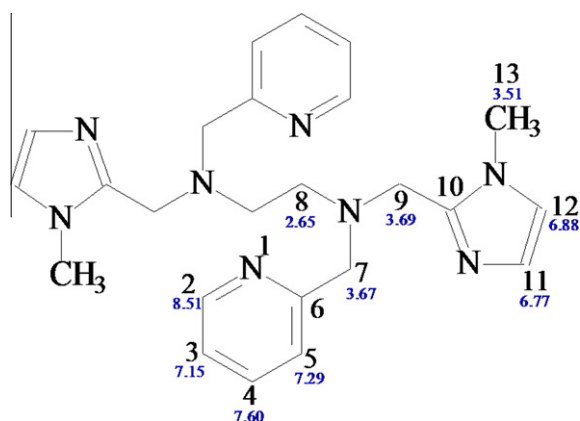
1		2	
Fe(1)–O(1)	1.852(1)	Fe(1)–O(1)	1.865(2)
Fe(1)–N(5)	2.094(2)	Fe(1)–N(6)	2.078(3)
Fe(1)–N(6)	2.095(2)	Fe(1)–N(5)	2.087(3)
Fe(1)–N(4)	2.263(2)	Fe(1)–N(4)	2.266(3)
Fe(1)–N(3)	2.272(2)	Fe(1)–N(3)	2.289(3)
Fe(1)–N(1)	2.381(2)	Fe(1)–N(2)	2.380(3)
Fe(1)–N(2)	2.394(2)	Fe(1)–N(1)	2.385(3)
O(1)–Fe(1)–N(5)	94.04(7)	O(1)–Fe(1)–N(6)	93.29(10)
O(1)–Fe(1)–N(6)	95.21(7)	O(1)–Fe(1)–N(5)	96.38(10)
N(5)–Fe(1)–N(6)	170.60(7)	N(6)–Fe(1)–N(5)	170.24(11)
O(1)–Fe(1)–N(4)	79.89(7)	O(1)–Fe(1)–N(4)	79.80(9)
N(5)–Fe(1)–N(4)	83.80(7)	N(6)–Fe(1)–N(4)	84.90(11)
N(6)–Fe(1)–N(4)	99.46(7)	N(5)–Fe(1)–N(4)	98.08(10)
O(1)–Fe(1)–N(3)	80.48(7)	O(1)–Fe(1)–N(3)	79.23(9)
N(5)–Fe(1)–N(3)	98.53(7)	N(6)–Fe(1)–N(3)	99.55(10)
N(6)–Fe(1)–N(3)	81.39(7)	N(5)–Fe(1)–N(3)	81.05(10)
N(4)–Fe(1)–N(3)	160.35(7)	N(4)–Fe(1)–N(3)	158.77(10)
O(1)–Fe(1)–N(1)	143.32(7)	O(1)–Fe(1)–N(2)	144.51(9)
N(5)–Fe(1)–N(1)	100.46(7)	N(6)–Fe(1)–N(2)	99.22(10)
N(6)–Fe(1)–N(1)	72.88(7)	N(5)–Fe(1)–N(2)	73.50(10)
N(4)–Fe(1)–N(1)	68.56(7)	N(4)–Fe(1)–N(2)	68.51(10)
N(3)–Fe(1)–N(1)	129.40(7)	N(3)–Fe(1)–N(2)	130.25(10)
O(1)–Fe(1)–N(2)	143.95(7)	O(1)–Fe(1)–N(1)	142.22(9)
N(5)–Fe(1)–N(2)	73.13(7)	N(6)–Fe(1)–N(1)	73.39(10)
N(6)–Fe(1)–N(2)	98.27(7)	N(5)–Fe(1)–N(1)	97.98(10)
N(4)–Fe(1)–N(2)	129.89(7)	N(4)–Fe(1)–N(1)	131.88(10)
N(3)–Fe(1)–N(2)	68.79(7)	N(3)–Fe(1)–N(1)	68.83(10)
N(1)–Fe(1)–N(2)	72.73(6)	N(2)–Fe(1)–N(1)	73.26(9)

where X[–] = ClO₄[–] or PF₆[–].

To a mixture of 0.0393 g (0.116 mmol) of Fe(BF₄)₂·6H₂O in methanol (10 mL) a solution of 0.05 g of dimpyen (0.116 mmol) was added drop-wise. The resulting orange solution was stirred 30 min, then slowly added 20 mL of methanol either with 0.057 g



Scheme 1. Synthetic route of the hexadentate ligand dimpyen.



Scheme 2. ^1H NMR chemical shifts of ligand dimpyen.

(0.349 mmol) of NH_4PF_6 for **1** or 0.05 g (0.35 mmol) of $\text{NaClO}_4 \cdot \text{H}_2\text{O}$ for **2**.

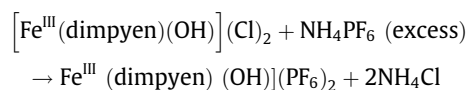
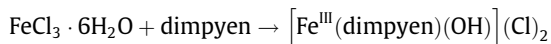
The final orange solution was left resting for 3 days and orange single crystals suitable for X-ray analysis were filtered off from the solution in both cases. A change in the oxidation state of the Fe(II) ion is observed, and a Fe(III) complex is obtained in both cases.

3.2.1.1. $[\text{Fe}^{\text{III}}(\text{dimpyen})(\text{OH})](\text{PF}_6)_2$ (**1**). Yield: 0.050 g, 54%. Orange crystals. FAB+MS: m/z 793 (M^+), 486 ($\text{M}-2\text{PF}_6-\text{OH}+\text{e}^-$), 648 ($\text{M}-\text{PF}_6$) $^+$. Anal. Calc. for $\text{C}_{24}\text{H}_{31}\text{N}_8\text{OP}_2\text{F}_{12}\text{Fe}$: C, 36.34; N, 14.12; H, 3.94. Found: C, 37.31; N, 13.50; H, 3.53%. MW : 793.33 g/mol.

3.2.1.2. $[\text{Fe}^{\text{III}}(\text{dimpyen})(\text{OH})](\text{ClO}_4)_2$ (**2**). Yield: 0.044 g, 54%. Orange crystals. FAB+MS: m/z 702 (M^+), 486 ($\text{M}-2\text{ClO}_4-\text{OH}+\text{e}^-$), 602 ($\text{M}-\text{ClO}_4$) $^+$. Anal. Calc. for $\text{C}_{24}\text{H}_{31}\text{N}_8\text{O}_9\text{Cl}_2\text{Fe}$: C, 41.02; N, 15.95; H, 4.42. Found: C, 41.57; N, 15.85; H, 4.25%. MW: 702.30 g/mol.

3.2.2. Synthesis with the Fe(III) salt

Using the Fe(III) salt gives the same complex. The synthetic procedure starting from the Fe(III) salt is depicted below:



To a mixture of 0.016 g (0.058 mmol) of $\text{FeCl}_3 \cdot 6\text{H}_2\text{O}$ in 10 mL of methanol was added drop-wise a solution of 0.025 g of dimpyen (0.058 mmol). The resulting orange solution was stirred 30 min then was slowly added 20 mL of methanol with 0.03 g (0.184 mmol) of NH_4PF_6 .

The final red solution was left at reduced pressure for a week and orange single crystals were filtered off from an orange solution and washed with water.

IR and MS data are essentially the same for both counteranions.

IR: 3448 cm^{-1} (O–H), 3086 cm^{-1} (CH aromatic ring) 2950 and 2892 cm^{-1} (C–H of CH_3 and CH_2), 1610 cm^{-1} (aromatic ring deformation), 1597 and 1572 cm^{-1} (imidazolic rings), 838 and 557 cm^{-1} (PF_6^- counterion).

4. Results and discussion

4.1. *N1,N2*-Di[(1-methyl-1*H*-2-imidazolyl)methyl]-*N1,N2*-di(2-pyridilmethyl)-1,2-ethanediamine ligand

This type of ligand was designed to modulate the properties of the metal ions bound to it. Due to the fact that the hexacoordinated tetrakis(2-pyridylmethyl)-1,2-ethanediamine iron (II) complex presents spin-crossover, a similar ligand with one pyridine exchanged with a benzyl substituent, produce Fe(II) complexes with very different properties but no spin-crossover, when these complexes are coupled to form a dimer with dicyanamide the obtained complex shows again the spin crossover-behavior [2]. The studied ligand has two pyridine rings exchanged by two methyl-imidazol rings in order to modify the character of the donor atom. A route with four steps has been envisioned to synthesize this new ligand, characterizing each intermediate. The global yield for the ligand was around 40% (see experimental).

4.2. Crystal structure of *N1,N2*-di[(1-methyl-1*H*-2-imidazolyl)methyl]-*N1,N2*-di(2-pyridilmethyl)-1,2-ethanediamine)hydroxo iron (III) hexafluorophosphate (**1**) and perchlorate (**2**)

The first point to note in the structure of both salts is that the Fe(III) ion, instead of being a regular hexacoordinated octahedron, has a quite rare heptacoordinated geometry. Additionally for the synthesis made starting from the iron (III) salt, the unit cell determined has the same values as the derivative obtained starting from the Fe(II) salt.

It is important to notice that there are very few examples of this geometry for Fe complexes and a search in the Cambridge Crystallographic Database results in only one example (a dimer) of the N_6O coordination system surrounding the Fe(III) center [18].

The structure consists of the $[Fe(dimpyen)OH]^{2+}$ cation units that comprise iron(III) centers coordinated to the hexadentate ligand dimpyen with one hydroxide in the coordination sphere. The Fe atom is heptacoordinated with N_6O environment by virtue of the six nitrogen atoms (N1, N2, N3, N4, N5 and N6) from chelating dimpyen ligand and an oxygen atom (O1) from hydroxide, forming a coordination polyhedron that can be described as a distorted pentagonal bipyramid. In general these heptadentate complexes can adopt any of three geometrical configurations, pentagonal bipyramidal, capped trigonal prism or capped octahedron. Since these geometries are energetically very similar it often acquires an intermediate geometry, as is this case [3]. A view of the perchlorate salt of the complex with atom numbering scheme is shown in Fig. 1.

Selected bond lengths and angles are summarized in Table 2. Considering the axis of the pentagonal bipyramid that with the largest angle, and the equatorial positions those nearest to the mean plane, it is observed that the two axial distances are shorter than the equatorial Fe–N bond, being N3 and N4 the pyridine, N5 and N6 the imidazole and N1 and N2 the olefinic nitrogen atoms, all of them more or less comparable to similar systems [19]. The Fe–O hydroxide bond length is the shortest of them all, as expected for this kind of bond. Fe1 is 0.010(1) Å for **1** and 0.014(1) for **2** out of the best equatorial plane defined by N1, N2, N3, N4 and O1 (the deviations from the mean plane are N1 = 0.544 (7), N2 = 0.548 (8), N3 = 0.331(8), N4 = 0.314 (8) and O1 = 0.013(8) Å for **1** and N1 = 0.505(7), N2 = 0.539(8), N3 = 0.354(8), N4 = 0.269(8) and O1 = 0.052(8) Å for **2**). The deviation from ideal pentagonal-bipyramidal geometry is indicated by the difference in the basal angles, which varies from 68.6(1)° to 80.5(1)° for **1** and 68.5(1)° to 79.8(1)° for **2**, while the axial sites are occupied by the nitrogen atoms from the imidazol moiety of the ligand yielding N5–Fe1–N6 as the trans-axial angle (170.61(8)° for **1** and 170.2(1)° for **2**). The coordination polyhedron is shown in Fig. S2 (supplementary material).

The unit cell consists of two $[Fe(dimpyen)OH]^{2+}$ units facing each other through the hydroxide, accompanied by two PF_6^- or two ClO_4^- anions for **1** and **2**, respectively (Fig. S1, unit cell of the perchlorate complex supplementary material). The Fe distances between nearest neighbors are 7.1416(7), 10.8778(8) and 16.109(1) Å for the hexafluorophosphate complex **1**, however although not very large there are differences for the perchlorate complex **2**, being the distances of the same neighbors at 6.8877(9), 9.104(1) and 9.330(1) Å. There are no true hydrogen bonds observed neither in **1** nor in **2**, and this explains the observed disorder in both the perchlorate and hexafluorophosphate moieties.

4.3. UV–Vis spectra of complexes **1** and **2**

Both compounds are soluble either in methanol or acetonitrile. The UV–Vis spectra of both complexes in acetonitrile solution were as expected virtually identical (see Fig. 2). The spectrum of **1** shows bands at 209 nm and at 258 nm which, by comparison with the spectrum of the free ligand dimpyen, are assigned to pyridinic and imidazolic rings $\pi \rightarrow \pi^*$ transitions, additionally the shoulder at 306 nm is assigned to a ligand–metal charge-transfer (LMCT) transition. In addition, a weaker and wide band is also observed and assigned to the charge transfer HO–Fe transition (λ_{max} at 404 nm with an extinction coefficient of 818 $cm^{-1} M^{-1}$). No bands at higher wavelengths are detected in the visible region.

The stability of the complex in solution is demonstrated by the unchanged absorbance along several hours for all the studied compounds, in spite that in general terms, the heptacoordinate $3d$ metal complexes are usually more labile than their corresponding octahedral species [20].

4.4. Magnetic properties of **1** and **2**

Compounds **1** (17 mg) and **2** (22 mg) are paramagnetic in all the studied temperature range. The magnetic behavior expressed as χT versus T , χ being the molar magnetic susceptibility and T the temperature, is shown in Fig. 3 for both compounds. The $\chi_M T$ product obtained at 300 K is nearly constant for both complexes within the

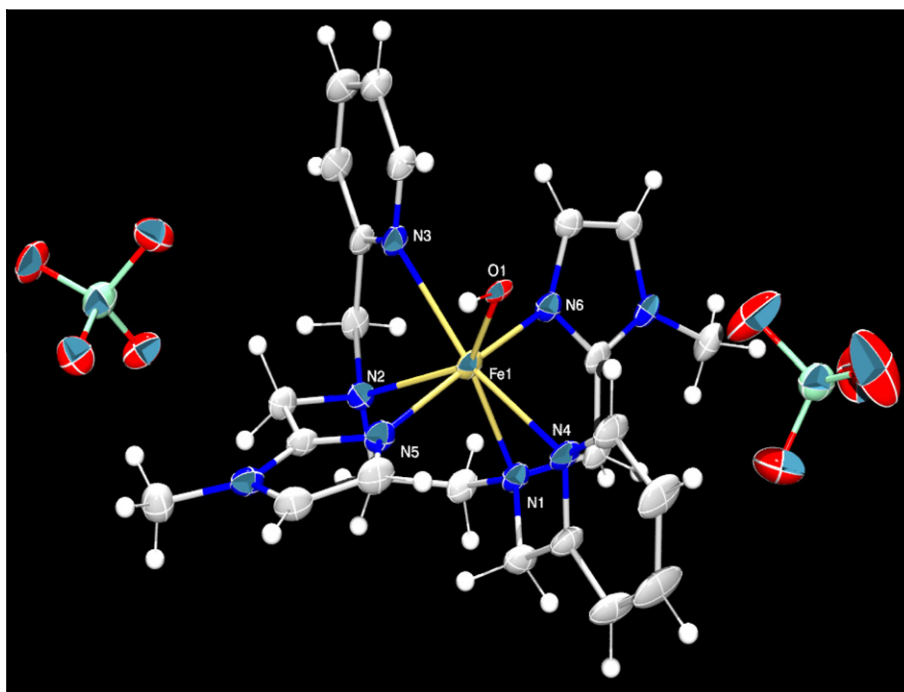


Fig. 1. ORTEP diagram of $[Fe(dimpyen)OH](ClO_4)_2$ (**2**) at 134 K with the corresponding atom numbering scheme. Displacement ellipsoids are shown at 50% probability levels.

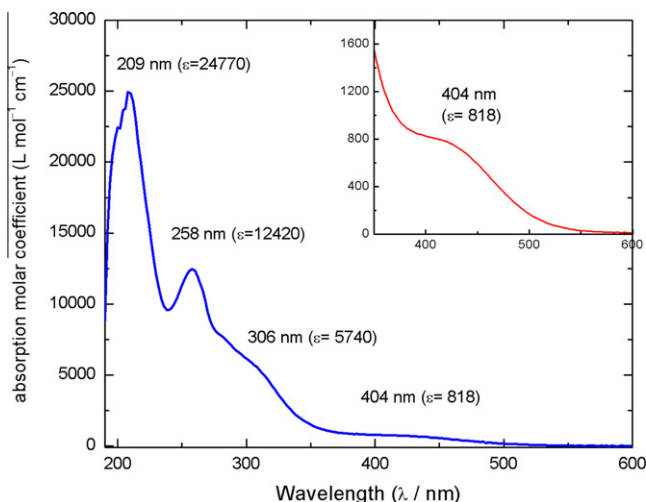


Fig. 2. UV-Vis spectra for $[\text{Fe}(\text{dimpyen})(\text{OH})](\text{PF}_6)_2$ (**1**) in CH_3CN solutions at 290 K obtained from 800 to 350 nm; concentration 1.6 mM.

temperature range explored, showing that the iron(III) remains high-spin ($S = 5/2$). The values obtained are $4.39 \text{ cm}^3 \text{ K mol}^{-1}$ for **1** and $4.34 \text{ cm}^3 \text{ K mol}^{-1}$ for **2**, with $\mu_{\text{eff}} = 5.9 \text{ BM}$ for both, which is in the range of the *spin-only* value, as expected for a Fe(III) ion [21].

4.5. Electrochemical properties

A typical voltammogram of the compounds is shown in Fig. 4, and presents a reversible signal at $E_{1/2} = -0.38 \text{ V}/\text{Fc}^+/\text{Fc}$, which can be attributed to a mono-electronic exchange process for the system Fe(III)/Fe(II). Additionally there is an irreversible signal at $E_{\text{cp}} = -1.45 \text{ V}/\text{Fc}^+/\text{Fc}$, that has been assigned to the reduction of the coordinated ligand dimpyen. The anodic sweep does not show any oxidation processes above $-0.38 \text{ V}/\text{Fc}^+/\text{Fc}$, while the cathodic sweep shows a reduction signal at $E_{\text{cp}} = -0.35 \text{ V}$ that can be assigned to the reduction from Fe(III) to Fe(II) in the coordination compound. This observation is consistent with the observed oxidation state of the metallic center in both compounds.

The half wave potential value for the Fe(III)/Fe(II) is $E_{1/2} = -0.38 \text{ V}/\text{Fc}^+/\text{Fc}$. This value is very small compared with those

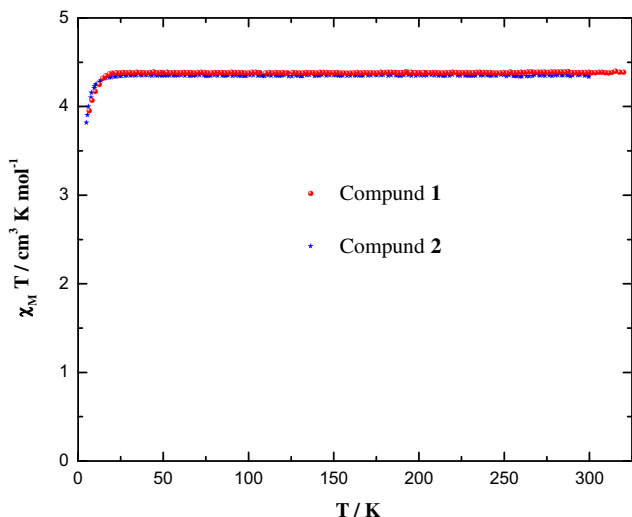


Fig. 3. Plot of $\chi_{\text{M}} T$ vs. T data for (a) **1** and (b) **2** compounds (rate of measurements: 1 K/min).

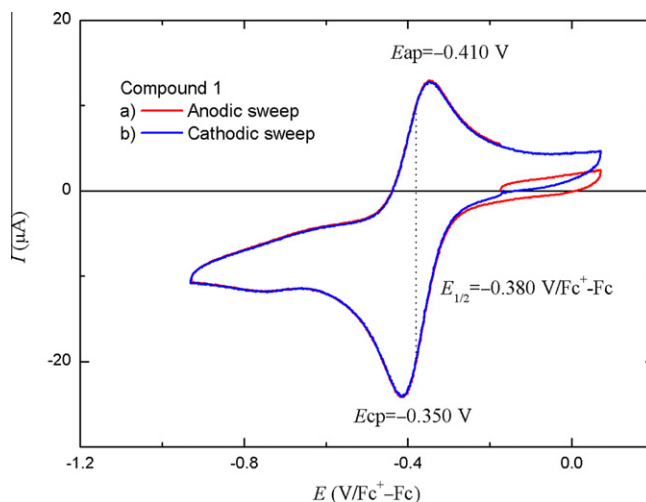


Fig. 4. Typical cyclic voltammograms of $[\text{Fe}(\text{dimpyen})(\text{OH})](\text{PF}_6)_2$ (**1**), obtained on carbon glass electrode in 0.1 M Bu_4NPF_6 CH_3CN solutions; recorded in (a) positive direction (anodic sweep) and (b) negative direction (cathodic sweep).

presented for similar complexes (0.576, 0.356, 0.350 $\text{V}/\text{Fc}^+/\text{Fc}$) [2] and can explain the reactivity of the Fe(II) in the coordination compound towards the molecular oxygen. The reason for this, stems from the fact that as the hydroxo complex is formed, the pH solution decrease as a result of the hydrolysis of the water bound to the Fe(II) at the same time, as the pH decrease the redox potential of the $\text{O}_2/\text{H}_2\text{O}$ pair increases, this favors the oxidation of Fe(II) to Fe(III). As the Fe(III) is formed, the hydrolysis of the water molecule is favored due to the higher acidity of Fe(III). As a consequence of this, the stability of the hydroxo complex of Fe(III) is enhanced and the redox potential of the Fe(III)/Fe(II) pair decrease, favoring symbiotically the global oxidation process. This can be observed in the reported $E_{1/2}$ value ($-0.38 \text{ V}/\text{Fc}^+/\text{Fc}$) of this system.

5. Conclusions

This paper shows the synthesis of a novel N_6 ligand and a rather rare heptacoordinated complex of Fe(III), in fact the only example to our knowledge of a simple Fe(III) N_6O complex. Even though the complex synthesis was started either with Fe(II) or Fe(III) salts, the end result was always the Fe(III) complex. This can be explained in terms of the ligand environment affecting the $E_{1/2}$ of the iron ion reacting with the molecular oxygen. Although the spin-crossover behavior was not observed, a small variation on the ligand, give off, a very important change in the redox properties of the system, promoting the formation of the Fe(III) heptadentate complex.

Acknowledgments

We are grateful to M. en C. Margarita Romero for her invaluable support on the characterization of the ligand, to Q. Marisela Gutierrez Franco for the IR spectra, to Georgina Duarte Lisci for the MS spectra and Nayeli López Balbiaux for the elemental analysis.

Appendix A. Supplementary material

CCDC 760507 and 760508 contain the supplementary crystallographic data for complexes **1** and **2**, respectively. These data can be obtained free of charge from The Cambridge Crystallographic Data Centre via www.ccdc.cam.ac.uk/data_request/cif. Supplementary data associated with this article can be found, in the online version, at [doi:10.1016/j.ica.2011.05.008](https://doi.org/10.1016/j.ica.2011.05.008).

References

- [1] P. Gütllich, Y. Garcia, H.A. Goodwin, *Chem. Soc. Rev.* 29 (2000) 419.
- [2] (a) N. Ortega-Villar, V.M. Ugalde-Saldivar, M.C. Muñoz, L.A. Ortiz-Frade, J.G. Alvarado-Rodríguez, J.A. Real, R. Moreno-Esparza, *Inorg. Chem.* 46 (2007) 7285;
(b) N. Ortega-Villar, A.L. Thompson, M.C. Muñoz, V.M. Ugalde-Saldivar, A.E. Goeta, R. Moreno-Esparza, J.A. Real, *Chem. Eur. J.* 11 (2005) 5721;
(c) X. Solans, L. Ruiz-Ramirez, R. Moreno-Esparza, M. Labrador, A. Escuer, *J. Solid State Chem.* 109 (1994) 315.
- [3] D. Casanova, P. Alemany, J.M. Bofill, S. Alvarez, *Chem. Eur. J.* 6 (2003) 1281.
- [4] K. Nakamoto, *Infrared and Raman Spectra of Inorganic and Coordination Compounds. Part B: Applications in Coordination, Organometallic and Bioinorganic Chemistry*, vol. 19, John Wiley, New York, 1997, p. 292.
- [5] J.R. Atwood, *Inorganic and Organometallic Reaction Mechanisms*, Wiley-VCH, New York, 1997.
- [6] (a) T. Schnepf, S. Seibig, A. Zahl, P. Tregloan, R. van Eldik, *Inorg. Chem.* 40 (2001) 3670;
(b) F.P. Rotzinger, *Chem. Rev.* 105 (2005) 2003.
- [7] (a) X.H. Bu, W. Chen, Z.H. Zhang, R.H. Zhang, S.M. Kuang, T. Clifford, *Inorg. Chim. Acta* 310 (2000) 110;
(b) P. Laine, A. Gourdon, J. Launay, J. Tuchagues, *Inorg. Chem.* 21 (1995) 5150;
(c) I. Morgenstern-Badarau, F. Lambert, J.P. Renault, M. Cesario, J.D. Marechal, F. Maseras, *Inorg. Chim. Acta* (1–2) (2000) 338;
(d) C.P. Raptopoulou, Y. Sanakis, A. Boudalis, *Eur. J. Inorg. Chem.* 36 (2008) 5632;
(e) F. Bonadio, M.C. Senna, J. Ensling, A. Sieber, A. Neels, H. Stoeckli-Evans, S. Decurtins, *Inorg. Chem.* 4 (2005) 969.
- [8] A. Majumder, G. Pilet, M.S.E. Fallah, J. Ribas, S. Mitra, *Inorg. Chim. Acta* 7 (2007) 2307.
- [9] D. Zhang, D.H. Busch, P.L. Lennon, R.H. Weiss, W.L. Neumann, D.P. Riley, *Inorg. Chem.* 5 (1998) 956. 963.
- [10] M.V. Cherrier, L. Martin, C. Cavazza, L. Jacquamet, D. Lemaire, J. Gaillard, J.C. Fontecilla-Camps, *J. Am. Chem. Soc.* 28 (2005) 10075. 10082.
- [11] G. Guisado-Barríos, Y. Li, A.M.Z. Slawin, D.T. Richens, I.A. Gass, P.R. Murray, L.J. Yellowlees, E.K. Brechin, *Dalton Trans.* (2008) 551.
- [12] G. Gritzner, J. Küta, *Pure Appl. Chem.* 4 (1984) 462.
- [13] A.J.C. Wilson (Ed.), *International Tables for Crystallography, Volume C*, Kluwer Academic Publishers, Dordrecht, The Netherlands, 1995.
- [14] R.C. Clark, J.S. Reid, *Acta Crystallogr., Sect. A* 51 (1995) 887.
- [15] C. Giacovazzo, M.C. Burla, R. Caliandro, M. Camalli, B. Carrozzini, G.L. Cascarano, L. De Caro, G. Polidori, R. Spagna, *SIR-2004 (v 1.0) A Program for Automatic Solution and Refinement of Crystal Structures*, 2004.
- [16] (a) G.M. Sheldrick, *SHELX97*, Programs for Crystal Structure Analysis, Release 97-2, Institut für Anorganische Chemie der Universität, Göttingen, Germany, 1998;
(b) G.M. Sheldrick, *Acta Crystallogr., Sect. A* 64 (2008) 112.
- [17] L. Farrugia, *ORTEP3 for Windows*, *J. Appl. Crystallogr.* 30 (1997) 565.
- [18] F.H. Allen, *Acta Crystallogr., Sect. B* 58 (2002) 380.
- [19] (a) J.M.D. Vera, J.S. Varela, I.B. Maimoun, E. Colacio, *Eur. J. Inorg. Chem.* (2005) 1907;
(b) D.S. Marlin, M.M. Olmstead, P.K. Mascharak, *Inorg. Chem.* 42 (2003) 1681;
(c) S.L. Jain, A.M.Z. Slawin, J.D. Woollins, P. Bhattacharyya, *Eur. J. Inorg. Chem.* (2005) 721;
(d) A. Majumder, C.R. Choudhury, S. Mitra, C. Marschner, J. Baumgartner, *Z. Naturforsch.* 60b (2005) 99;
(e) X. Wang, S. Wang, L. Li, E.B. Sundberg, G.P. Gacho, *Inorg. Chem.* 42 (2003) 7799;
(f) J.D. Lee, M.H. Lee, *J. Ind. Eng. Chem.* 7 (2001) 137.
- [20] I. Ivanović-Burmazović, M.S.A. Hamza, R. van Eldik, *Inorg. Chem. Commun.* 11 (2002) 937.
- [21] O. Kahn, *Molecular Magnetism*, VCH, Weinheim, 1993.